

Morphology Control of Various Aromatic Polyimidazoles—Preparation of Nanofibers

Jin Gong,¹ Tetsuya Uchida,² Shinichi Yamazaki,¹ Kunio Kimura¹

¹Graduate School of Environmental Science, Okayama University, Okayama 700-8530, Japan

²Graduate School of Natural Science and Technology, Okayama University, Okayama 700-8530, Japan

Received 12 August 2010; accepted 29 November 2010

DOI 10.1002/app.33914

Published online 29 March 2011 in Wiley Online Library (wileyonlinelibrary.com).

ABSTRACT: Morphology of four kinds of aromatic polyimidazoles was examined by using reaction-induced crystallization during solution polymerization at a concentration of 1% at 350°C in liquid paraffin (LPF), dibenzyltoluene (DBT), and the mixture of these solvents. Aggregates of ribbon-like crystals of poly[2,6-(2,6-naphthalene)-benzobisimidazole] were obtained in LPF, and those of plate-like crystals were obtained in DBT/LPF-50 and in DBT. In contrast to this, the network structures of poly[2,2'-(2,6-naphthalene)-5,5'-bibenzimidazole] (PNT-BBI) nanofibers with the diameter of 25 to 90 nm was mainly obtained in DBT. The network structures of the PNT-BBI nanofibers could be recognized as nonwoven fabrics of the high-performance polymers. Imidazole trimers were precipitated to form the ribbon-like crystals and then they were continuously supplied from solution to grow

the crystals. Molecular weight increased by the polymerization on the surface of the crystals when they crystallized and in the crystals. The initially formed aggregates of ribbon-like crystals changed to the nanofibers with time. In the case of poly[2,6-(4,4'-biphenylene)-benzobisimidazole] and poly[2,2'-(4,4'-biphenylene)-5,5'-bibenzimidazole], they exhibited various morphologies such as spheres, lath-like crystals, and the spherical aggregates of lath-like crystals depending on the solvent, but fibers like PNT-BBI were not formed. The crystals obtained in this study possessed very high crystallinity and the outstanding thermal stability measured by TGA. © 2011 Wiley Periodicals, Inc. *J Appl Polym Sci* 121: 2851–2860, 2011

Key words: crystallization; fibers; high performance polymers; morphology; polyimidazole

INTRODUCTION

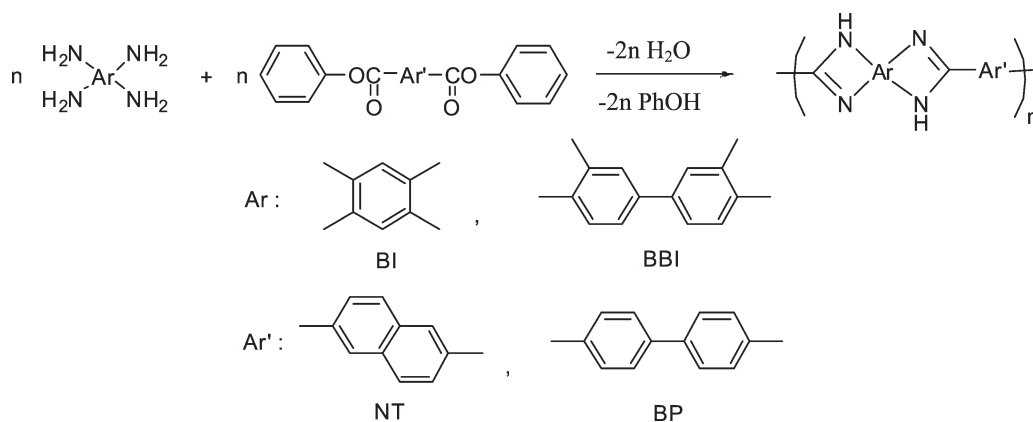
Wholly aromatic polyimidazoles are a class of high-performance heterocyclic polymers. They have widespread potential applications in high-performance protective, semiconductor, electronics, and other high-technological fields^{1–11} due to their outstanding chemical resistance, mechanical strength, radiation stability, especially for their superior thermal stability and flame retardant.^{12–21} It was found in the last decades that materials down-sized to the nanometer scale can show very different properties, enabling unique applications.^{23,24} Nanofibers are more indispensable to obtain essential properties of polymers in high-technological field. However, the fully aromatic nature and stiffness of molecular chains of polyimidazoles not only endue them with superior properties, but also bring about their poor solubility and infusibility.²⁵ This intractability causes the mor-

phology control of wholly aromatic polyimidazoles in nanometer-scale difficult by physical processing technique like electrospinning and others.

Isothermal polymerizations can induce phase separation from homogeneous solution^{26–31} and the reaction-induced phase separation during isothermal solution polymerization is a very useful method for the morphology control of poor processable polymers, because the morphology is created by the phase-separation of oligomers.^{32,33} This method is not limited by the processability of polymers. In our previous works, the morphology control of the following four aromatic polyimidazoles had been examined by the reaction-induced crystallization during polymerization; poly[2,2'-(1,3-phenylene)-5,5'-bibenzimidazole], poly[2,2'-(1,4-phenylene)-5,5'-bibenzimidazole], poly[2,6-(1,4-phenylene)-benzobisimidazole], and poly(2,5-benzimidazole).^{34–37} Among them the latter three polyimidazoles afforded the nanofibers. There still remains what kinds of polyimidazole afford the nanofibers. To prepare other polyimidazole nanofibers, this study examined the morphology control of various fully aromatic polyimidazoles containing 2,6-naphthalene moiety and 4,4'-biphenylene moiety, which were poly[2,6-(2,6-naphthalene)-benzobisimidazole] (PNT-BI), poly[2,2'-(2,6-naphthalene)-5,5'-bibenzimidazole] (PNT-BBI),

Correspondence to: K. Kimura (polykim@cc.okayama-u.ac.jp).

Contract grant sponsor: Ministry of Education, Culture, Sports, Science and Technology, Japan; contract grant number: 21350127.



Scheme 1 Synthesis of aromatic polyimidazoles.

poly[2,6-(4,4'-biphenylene)-benzobisimidazole] (PBP-BI) and poly[2,2'-(4,4'-biphenylene)-5,5'-bibenzimidazole] (PBP-BBI), using reaction-induced crystallization of oligomers as depicted in Scheme 1.

EXPERIMENTAL

Materials

The chemical 1,2,4,5-tetraaminobenzene tetrahydrochloride (TAB 4HCl) was purchased from Sigma-Aldrich Co. Ltd. (St. Louis) and recrystallized from deaerated water. 1,2,4,5-Tetraaminobenzene (TAB) was prepared from TAB 4HCl according to a previous procedure.¹ 3,3'-Diaminobenzidine (DAB) was purchased from Sigma-Aldrich Co. Ltd. (St. Louis) and recrystallized from methanol with a small amount of activated charcoal. Phenol, biphenyl-4,4'-dicarboxylic acid (BPA) and naphthalene-2,6-dicarboxylic acid (NTA) were purchased from TCI Co. Ltd. (Tokyo, Japan) and used as received. Thionyl chloride was purchased from Nakalai Tesque Inc. (Kyoto, Japan). Triethylamine was purchased from Sigma-Aldrich Co. Ltd. (St. Louis). A mixture of structural isomers of dibenzyltoluene (DBT) was purchased from Matsumura oil Co. Ltd. (Trade name was Barrel Therm 400, MW: 380, bp: 382°C) (Osaka, Japan) and purified by vacuum distillation (180–200°C/0.3 mmHg). Liquid paraffin (LPF) was purchased from Nacalai Tesque Co. Ltd. (Kyoto, Japan) and purified by vacuum distillation (220–240°C/0.3 mmHg).

Characterization

Infrared (IR) spectra were recorded on a JASCO FT/IR-410 spectrometer (Tokyo, Japan). The proton nuclear magnetic resonance (¹H-NMR) spectra were recorded on a 300-MHz FT-NMR system (AL-300, JEOL) (Tokyo, Japan). Differential scanning calorimeter (DSC) was performed on a Perkin-Elmer DSC

8000 (Waltham, MA) with a heating rate of 20°C·min⁻¹ in nitrogen. Inherent viscosity (η_{inh}) was measured in 97% sulfuric acid at a concentration of 0.2g·dL⁻¹ at 30°C. Morphologies and sizes of the products were observed on a Hitachi S-3500N scanning electron microscope (SEM) (Tokyo, Japan). Samples for SEM observation were dried, sputtered with platinum/palladium, and observed at 20 kV. Average size parameters of the products were determined by taking the average of over 150 observation values. Thermogravimetric analysis (TGA) (Waltham, MA) was performed on a Perkin-Elmer TGA-7A with a heating rate of 20°C·min⁻¹ in nitrogen. Wide angle X-ray scattering (WAXS) was performed on a RIGAKU MiniFlex diffractometer (Matsumoto, Japan) with nickel-filtered Cu-K α radiation at a scanning rate of 1 degree min⁻¹. Matrix assisted laser desorption ionization time-of-flight (MALDI-TOF) mass spectrometry were performed on a Bruker Daltonics AutoFLEX MALDI-TOF MS system (Billerica, MA) operating with a 337-nm N₂ laser. Spectra were obtained in the linear positive mode with an accelerating potential of 20 kV. Mass calibration was performed with angiotensin I (MW 1296.69) and insulin B (MW 3496.96) from a Sequazyme peptide mass standard kit. Samples were prepared by the evaporation-grinding method and ran in 3-aminoquinoline as a matrix doped with potassium trifluoroacetate (KFTA) according to previously reported procedures.³⁸

Synthesis of diphenyl naphthalene-2,6-dicarboxylate (DPNT)

Into a four-neck round-bottom flask equipped with nitrogen inlet/outlet tubes were placed NTA (10 g, 46.3 mmol), thionyl chloride (40 mL), *N,N*-dimethylformamide (1.0 mL), and dehydrated toluene (100 mL). The mixture was refluxed for 3 h under stirring and a slow nitrogen flow. After the orange liquid phase was removed, the colorless liquid phase was

cooled to 25°C and white needle crystals of naphthalene-2,6-dicarbonyl dichloride (NTA-Cl) were precipitated. They were collected by filtration and dried under reduced pressure at 25°C for 24 h yielding 9.56 g (81%). Phenol (7.06 g, 75.0 mmol) was added to a solution of NTA-Cl (9.56 g, 37.5 mmol) in 250 mL of dehydrated tetrahydrofuran (THF). The mixture was allowed to cool at 0°C and a solution of triethylamine (15.67 mL, 112.5 mmol) in 50 mL of THF was added dropwise into the mixture under stirring at 0°C. Then the mixture was stirred at 0°C for 3 h and 25°C for 12 h. Precipitates were collected by filtration, washed with water and then dried. Recrystallization from toluene/methanol yielded 7.32 g (53%) of DPNT as white crystals. Total yield: 70%, mp: 218–219°C. IR (KBr, cm^{-1}): 3450, 3058, 1785, 1731, 1695, 1592, 1491, 1455, 1372, 1338, 1296, 1279, 1260, 1215, 1187, 1162, 1140, 1079, 1023, 1004, 971, 926, 904, 836, 830, 758, 737, 688, 489. $^1\text{H-NMR}$ (300 MHz, $\text{DMSO-}d_6$, ppm): 8.98 (s, 2H), 8.45–8.36 (d, $J = 8.62$ Hz, 2H), 8.28–8.20 (d, $J = 8.61$ Hz, 2H), 7.56–7.46 (m, 4H), 7.40–7.30(m, 6H).

Synthesis of diphenyl biphenyl-4,4'-dicarboxylate (DPBP)

DPBP was synthesized by the similar procedures of DPNT. Total yield: 72%, mp: 213–214°C. IR (KBr, cm^{-1}): 3443, 3058, 1730, 1608, 1593, 1494, 1456, 1396, 1331, 1286, 1267, 1209, 1160, 1131, 1087, 1022, 1001, 918, 856, 843, 749, 692, 510. $^1\text{H-NMR}$ (300 MHz, $\text{DMSO-}d_6$, ppm): 8.32–8.23 (d, $J = 8.61$ Hz, 4H), 8.09–8.00 (d, $J = 8.25$ Hz, 4H), 7.56–7.46 (m, 4H), 7.38–7.28 (m, 6H).

Polymerization

Polymerization of PNT-BI in DBT at a concentration of 1% (the calculated theoretical polymer weight/the solvent weight) was described as a typical example. DPNT (0.26 g, 35.4 mmol) and DBT (20 g) were placed into a cylindrical flask equipped with gas inlet and outlet tubes and was heated up to 350°C under slow stream of nitrogen. When the temperature reached to 350°C, TAB (0.10 g, 35.4 mmol) was added into the solution. The mixture was stirred for 5 s to dissolve TAB, and then polymerization was carried out for 6 h at 350°C without stirring. Precipitated polymers were isolated by filtration at 350°C to avoid the precipitation of oligomers, and then washed with acetone; 0.12 g (62%) of PNT-BI crystals was obtained. A filtrate was poured into toluene and the precipitated oligomers which were dissolved in DBT at 350°C were collected by filtration. Other polymerizations were carried out in the similar manner.

RESULTS AND DISCUSSION

Morphologies of aromatic polyimidazoles

Solvents poor to the polymer and good to the monomer are required to induce phase separation of oligomers during solution polymerization. Morphology of the precipitates is significantly influenced by the solubility of oligomers.³⁸ Hence, LPF, DBT, and the mixture of LPF and DBT (DBT/LPF-50, the number stands for weight percent of LPF, similarly hereinafter) were used as the solvent for the polymerization. Polymerizations were carried out at a concentration of 1% at 350°C for 6 h. Monomers were insoluble into the solvents at 25°C, but they became dissolved at 350°C. The solution became turbid in the initial stage of polymerization due to the precipitation of oligomers and then the precipitates were obtained after 6 h. Table I presents the results of the polymerization and Figure 1 shows the morphologies of the precipitates.

As for PNT-BI, the aggregates of ribbon-like crystals were obtained in LPF (run no. 1) with the yield of 42% as shown in Figure 1(a). The size of ribbon-like crystals is 150 to 300 nm in thickness and 0.6 to 1.0 μm in width. The surface of ribbon-like crystals is rugged and covered with 100 to 250 nm of granules. Aggregates of thin plate-like crystals were obtained in DBT/LPF-50 (run no. 2) with the yield of 42%, of which the thickness was ~ 100 nm. Aggregates of plate-like crystals were also obtained in DBT (run no. 3) with the yield of 62% and the thickness of the plate-like crystals was ~ 50 nm as shown in Figure 1(b). PNT-BI was dissolved only in sulfuric acid, and therefore the inherent viscosity (η_{inh}) measured in 97% sulfuric acid was used to evaluate molecular weight. The value of η_{inh} of the obtained PNT-BI crystals were 0.40 to 0.42 $\text{dL}\cdot\text{g}^{-1}$ and there was not large difference between the solvents. Chemical structure of the obtained crystal was confirmed by IR spectroscopy, and that of PNT-BI prepared in run no. 3 was presented in Figure 2(a) as a representative. Characteristic peaks of the imidazole ring were clearly visible at 3450 to 3000 cm^{-1} (N-H and aromatic C-H stretching), 1630 cm^{-1} (C = N stretching), 1280 cm^{-1} (C-N stretching), and 820 cm^{-1} (N-H stretching) which is identical with the PNT-BI. Figure 3(a) shows the WAXS intensity profile of PNT-BI crystals prepared in run no. 3. Six sharp peaks were clearly observed at 2θ of 17.97° (d -spacing = 0.493 nm), 19.50°(0.455 nm), 21.12°(0.420 nm), 23.46°(0.379 nm), 26.58°(0.335 nm), and 28.26°(0.316 nm), and the crystals possessed high crystallinity. As for the other polyimidazoles containing 2,6-naphthalene moiety, polymerizations of PNT-BBI were carried out at a concentration of 1% and 350°C for 6 h in five different solvents; LPF, DBT/LPF-70, DBT/LPF-50, DBT/LPF-30, and DBT.

TABLE I
Polymerization Results of Various Polyimidazoles^a

Run no.	Polymer code	Solvent	Yield (%)	η_{inh}^b (dL·g ⁻¹)	Morphology	$T_{10\%}^c$ (°C)
1	PNT-BI	LPF	42	0.40	Ribbon	449
2	PNT-BI	DBT/LPF-50	42	0.40	Plate	511
3	PNT-BI	DBT	62	0.42	Plate	540
4	PNT-BBI	LPF	56	0.45	Sphere	593
5	PNT-BBI	DBT/LPF-70	65	0.54	Needle	642
6	PNT-BBI	DBT/LPF-50	61	0.61	Ribbon	642
7	PNT-BBI	DBT/LPF-30	51	0.63	Fiber, ribbon	585
8	PNT-BBI	DBT	52	0.67	Fiber, ribbon	594
9	PBP-BI	LPF	41	0.51	Plate	483
10	PBP-BI	DBT/LPF-50	50	0.50	Plate	491
11	PBP-BI	DBT	75	0.45	Plate	568
12	PBP-BBI	LPF	22	0.71	Sphere	727
13	PBP-BBI	DBT/LPF-50	18	0.68	Sphere, lath	702
14	PBP-BBI	DBT	24	0.61	Lath	690

^a Polymerizations were carried out at 350°C at a concentration of 1.0% for 6 h.

^b The inherent viscosity (η_{inh}) was measured in 97% sulfuric acid at a concentration of 0.2 g·dL⁻¹ at 30°C.

^c Temperature of 10% weight loss measured on a TGA at a heating rate of 20°C·min⁻¹ in N₂.

Spherical aggregates of fine crystals were formed in LPF (run no. 4) with the yield of 56% as shown in Figure 1(c). This spherical morphology suggests that they were possibly formed via the liquid-liquid phase separation rather than crystallization due to the lower molecular weight of the precipitated oligomers in LPF as discussed later with the results of MALDI-TOF mass spectrometry. In contrast with this, the polymerization in DBT/LPF-70 (run no. 5) afforded aggregates of needle-like crystals with the yield of 65% as shown in Figure 1(d) and spherical aggregates of fine crystals disappeared. Their width and length were 0.7-1.5 μm and 2.5 to 5.0 μm , respectively. The needle-like crystals grew from a center point and the trace of the pilling up structure of lamellae was observed along the long axis of the needle. The needle-like crystals have a higher η_{inh} of 0.54 dL·g⁻¹ than that of spherical aggregates prepared in LPF. Morphology of the precipitates changed drastically in the solvent containing DBT. Ribbon-like crystals covered with many needle-like crystals on the surface were obtained with the yield of 61% in DBT/LPF-50 (run no. 6) as shown in Figure 1(e). The ribbon-like crystals have the size of 400-800 nm in width and 5 to 10 μm in length. The needle-like crystals have the size of \sim 50 nm in diameter and 100-150 nm in length. In DBT/LPF-30 (run no. 7), fibers having the diameter of 30 to 80 nm shown in Figure 1(f) and ribbon-like crystals having the width of 100 to 500 nm shown in Figure 1(g) were formed with the yield of 51%. The former has the dominant share and the latter is a little. It is impossible to estimate the fiber length for the aggregation of fibers. The ribbon-like crystals also seem

likely to be the bundle of many fibers. In DBT (run no. 8), fibers having the diameter of 25 to 90 nm were obtained as shown in Figure 1(h) with small amount of aggregations of plate crystals with the yield of 52%. Fibers entangled each other and the length is also unable to estimate. All the obtained PNT-BBI crystals have high η_{inh} from 0.45 to 0.67 dL·g⁻¹ and the fibers prepared in DBT have the highest η_{inh} of 0.67 dL·g⁻¹. Figure 2(b) is the IR spectrum of the fibers prepared in run no. 8. The characteristic peaks of imidazole rings are also clearly observed and the formation of PNT-BBI is confirmed. The WAXS intensity profiles of PNT-BBI nanofibers prepared in run no. 8 are shown in Figure 3(b). Although the profiles contained broad halo attributed to amorphous region, three sharp peaks were observed at 2θ of 19.21° (0.462 nm), 20.96° (0.424 nm), and 27.36° (0.326 nm), and this profile indicates that the PNT-BBI nanofibers exhibit high crystallinity.

Next, the polymerization of the polyimidazoles containing 4,4'-biphenylene moiety was examined. PBP-BI plate crystals having smooth surfaces with the yield of 41 and 75% were formed in both LPF and DBT (run no. 9 and 11) as shown in Figure 4(a,b). The thickness of the former was 50 to 120 nm, about 2.5 times thicker than the latter of 20 to 50 nm. In mixed solvent DBT/LPF-50 (run no. 10), plate crystals were also obtained with the yield of 50%. Their thickness ranged from 80 nm to 200 nm. The chemical structure was analyzed by IR spectroscopy, and Figure 2(c) shows that of plate crystals prepared in run no. 11. Characteristic peaks of imidazole ring were also clearly observed to confirm the formation

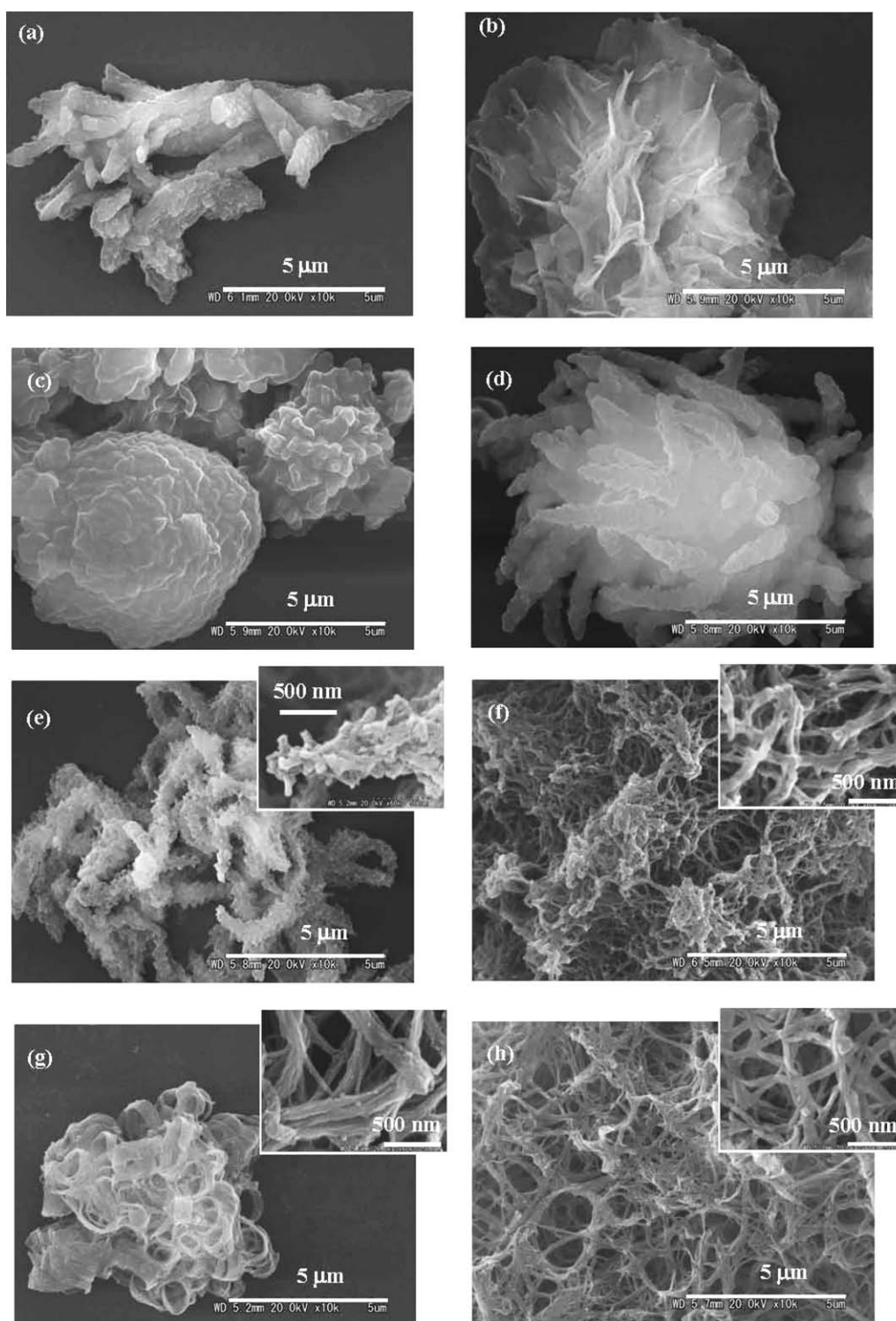


Figure 1 Morphologies of PNT-BI crystals prepared in (a) LPF (run no. 1), (b) DBT (run no. 3), and PNT-BBI crystals prepared in (c) LPF (run no. 4), (d) DBT/LPF-70 (run no. 5), (e) DBT/LPF-50 (run no. 6), (f, g) DBT/LPF-30 (run no. 7), and (h) DBT (run no. 8).

of PBP-BI. The crystallization property was estimated by the WAXS profile of the plate crystals obtained in LPF and DBT. Three sharp peaks at 2θ of 20.10° , 23.68° , and 28.85° were observed and these crystals possess very high crystallinity. PBP-BI was

dissolved only in sulfuric acid, and therefore the η_{inh} measured in 97% sulfuric acid was also used to evaluate molecular weight. The value of η_{inh} of PBP-BI plate crystals were 0.45 to $0.51 \text{ dL}\cdot\text{g}^{-1}$ and the molecular weights of the precipitates are speculated

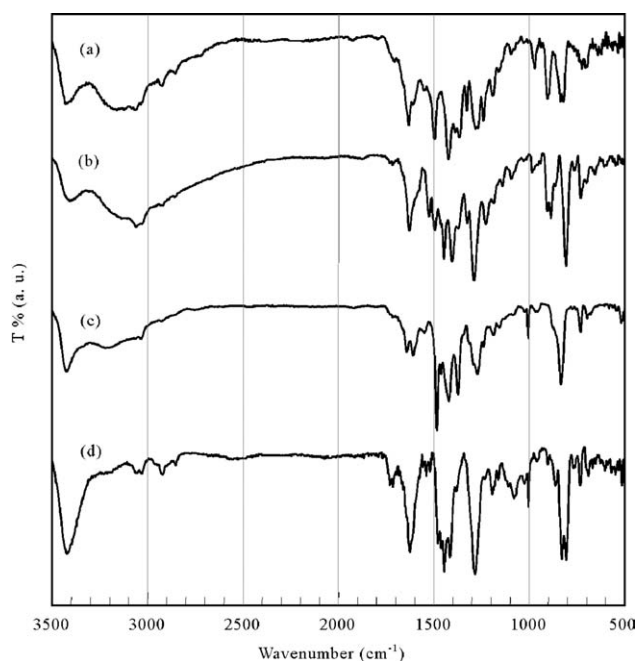


Figure 2 IR spectra of (a) PNT-BI (run no. 3), (b) PNT-BBI (run no. 8), (c) PBP-BI (run no. 11), and (d) PBP-BBI (run no. 14)

high. As for PBP-BBI, spheres were obtained in LPF with the yield of 22% as shown in Figure 4(c). The diameter of spheres was 3.0 to 6.0 μm . Both spheres and lath-like precipitates were obtained with the yield of 18% in DBT/LPF-50. In DBT, the spherical aggregates of lath-like crystals were obtained with the yield of 24%, which had the size of 10 to 20 μm as shown in Figure 4(d). The size of the lath-like crystals were 100 to 500 nm in thickness, 0.3 to 2.5 μm in width, and 2.0 to 20 μm in length. Interestingly, the lath-like crystals grew radially from the center point and this unique morphology resembles the spherulites. The IR spectrum and the WAXS intensity profile of the spherical aggregates of lath-like PBP-BBI crystals was shown in Figures 2(d) and 3(e), respectively. Characteristic peaks of polyimidazoles were clearly observed to confirm the formation of PBP-BBI. In the WAXS profile, although the profiles contained broad halo attributed to amorphous region, five sharp peaks were observed at 19.39° (0.457 nm), 20.67° (0.429 nm), 24.37° (0.365 nm), 26.59° (0.335 nm), and 29.19° (0.306 nm). This indicates that the PBP-BBI precipitates also have significantly high crystallinity. The η_{inh} of the prepared PBP-BBI was 0.61 to 0.71 $\text{dL}\cdot\text{g}^{-1}$, suggesting that the prepared PBP-BBI have very high molecular weight.

Thermal stability of the obtained crystals was measured on TGA in nitrogen. TGA curves of PNT-BI (run no. 3), PNT-BBI (run no. 8), PBP-BI (run no. 11), and PBP-BBI (run no. 14) were shown in Figure 5 as examples. Thermal decomposition of these poly-

mers seems complicated and multi-step decomposition behaviors were observed in TGA curves. PNT-BI which was nanofibers was stable up to 400°C , but others exhibited several % weight loss at ca 250 to 300°C . The weight loss at lower temperature is likely caused by low molecular weight oligomers. Among them, PNT-BBI nanofibers possessed the highest thermal stability due to high crystallinity and high molecular weight. The 10% weight loss temperatures ($T_{10\%}$) were presented in Table I. The values of $T_{10\%}$ of the PNT-BI crystals ranged from 449 to 540°C , and those of the PNT-BBI were higher than those of PNT-BI in the range of 585 to 642°C . The values of $T_{10\%}$ of the PBP-BI plate crystals ranged from 483 to 568°C , and those of the PBP-BBI ranged from 609 to 727°C . The polyimidazoles prepared from BBI were more thermally stable than those prepared from BI, and PBP-PPIs were the most stable among them. These aromatic polyimidazoles do not exhibit melting behavior under their decomposition. Therefore, the value of $T_{10\%}$ is influenced by various factors such as molecular weight, distribution of molecular weight, crystallinity, morphology, surface area, structure of end-group, and so on besides molecular structure. The network structures of the PNT-BBI nanofibers exhibited good thermal stability, but an obvious relationship between morphology and thermal stability was not obtained in the series of the obtained polyimidazoles.

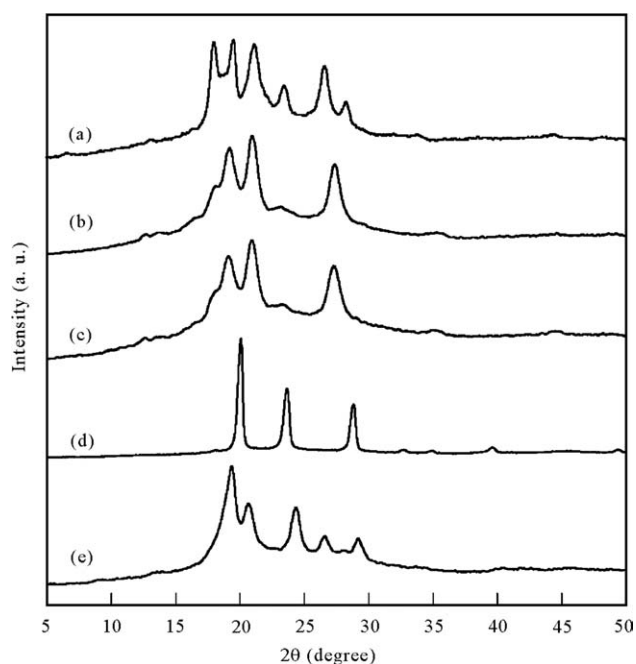


Figure 3 WAXS intensity profiles of various polyimidazoles prepared in DBT at a concentration of 1% at 350°C . (a) PNT-BI for 6 h (run no. 3), (b) PNT-BBI for 6 h (run no. 8) and (c) for 1.5 h, (d) PBP-BI for 6 h (run no. 11), (e) PBP-BBI for 6 h (run no. 14).

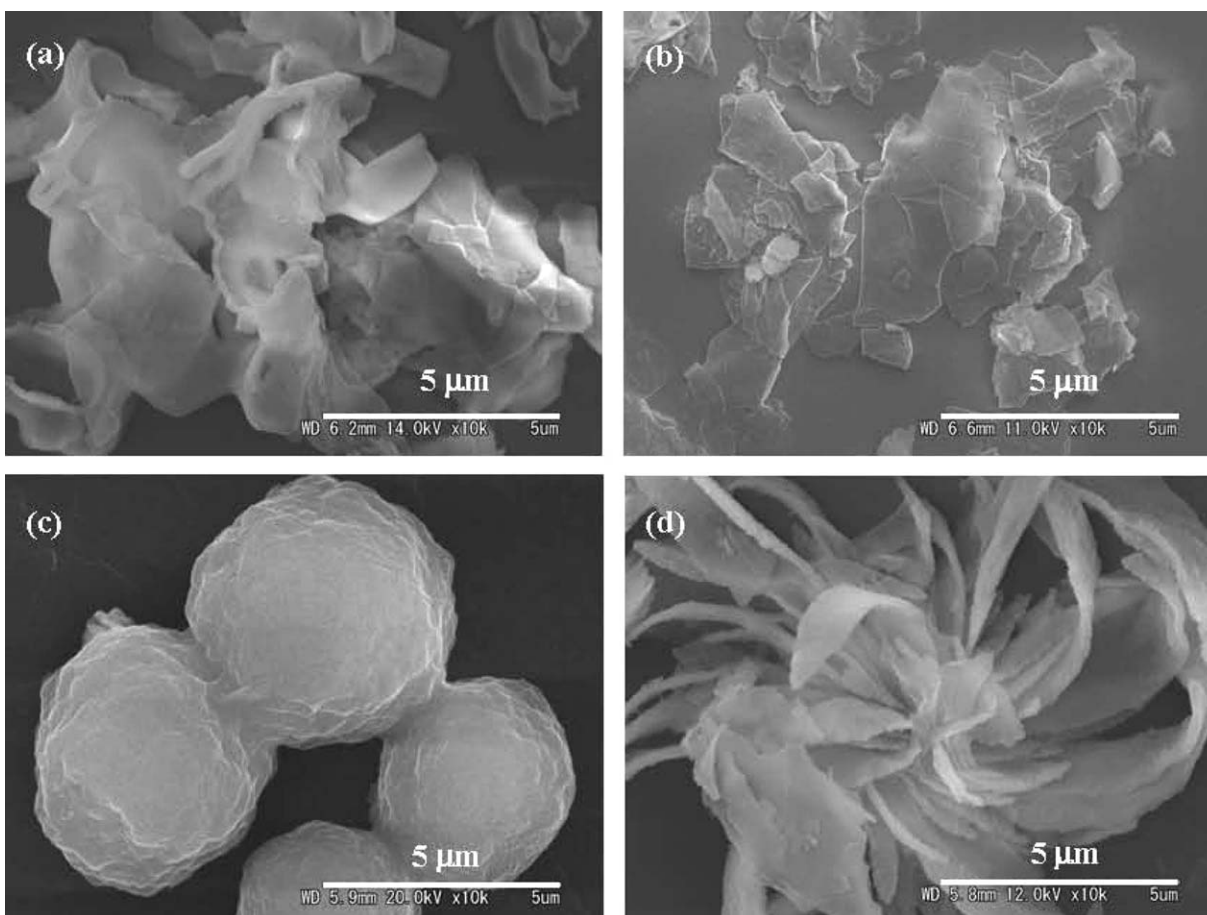


Figure 4 Morphologies of PBP-BI crystals prepared in (a) LPF (run no. 9), (b) DBT (run no. 11) and PBP-BBI crystals prepared in (c) LPF (run no. 12), (d) DBT (run no. 14).

Formation mechanism of PNT-BBI nanofibers

Among four aromatic polyimidazoles, only PNT-BBI afforded the network structure of the nanofibers. To clarify the formation of the PNT-BBI nanofibers, the changes in the morphology, the yield, and the inherent viscosity of the precipitated crystals were investigated in the course of polymerization in DBT. The results are shown in Figure 6. Precipitation of oligomers started after 35 min and the yield increased significantly with time until 3.5 h. Then it increased slightly afterward. Correspondingly, the values of η_{inh} increased significantly from 0.06 to $0.56 \text{ dL}\cdot\text{g}^{-1}$ until 3.5 h. Then it increased continuously with time and reached to $0.67 \text{ dL}\cdot\text{g}^{-1}$ of after 6 h. Oligomers left in DBT at 350°C were collected from the solution after 6 h, and analyzed by MALDI-TOF mass spectrometry. The spectrum is shown in Figure 7(a) and the peaks are identified as listed in Table II. The oligomers up to dimmers were detected and many of them were cyclized. This result implies that cyclized imidazole trimers were mainly precipitated to form the crystals. Based on these, it can be concluded that the cyclized imidazole trimers are supplied consecutively from solution

to form the crystals, and the molecular weight increases by the polymerization on the surface of the crystals and in the crystals. Aggregates of ribbon-like crystals were formed after 1.5 h. Then they changed to the fibers until 2.5 h, of which the

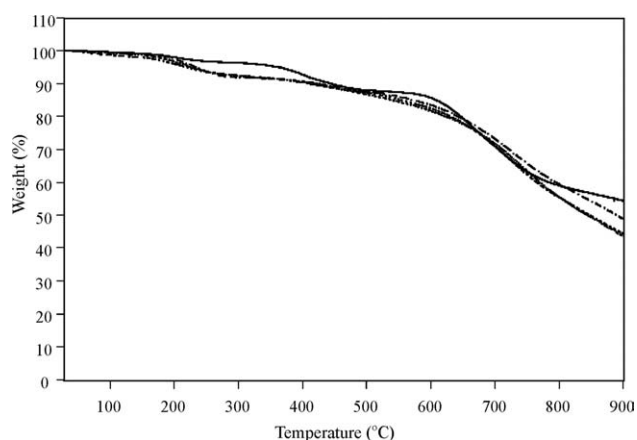


Figure 5 TGA curves of various polyimidazoles prepared in DBT at a concentration of 1% and 350°C for 6 h. (a) PNT-BI (run no. 3) (dashed line), (b) PNT-BBI (run no. 8) (solid line), (c) PBP-BI (run no. 11) (dotted line), and (d) PBP-BBI (long dashed short dashed line).

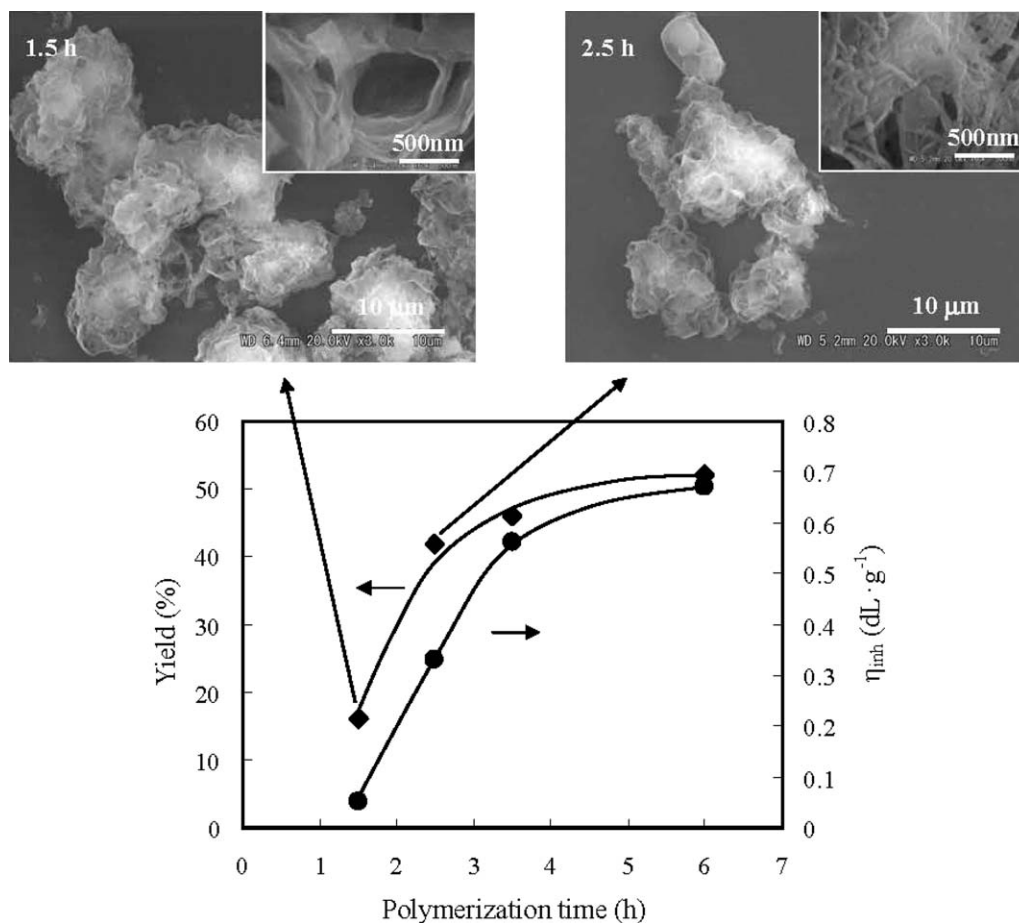


Figure 6 Morphologies, and plots of yield (◆) and inherent viscosity (●) of PNT-BBI crystals prepared in DBT as a function of polymerization time.

diameter of the fibers was from 25 to 90 nm corresponding to that prepared for 6 h. Although the reason why the ribbon-like crystals reorganized to the fine fiber crystals is not exactly clear so far, the observed ribbon-like structure might be the initial structure of the final fibers. The WAXS profiles of PNT-BBI precipitates prepared for 1.5 h is shown in Figure 3(c). Diffraction peaks of PNT-BBI precipitates prepared for 1.5 h were as sharp as that of prepared for 6 h, indicating the crystallinity of the crystals prepared for 1.5 h was as quite high as that for 6 h. The average crystallite size was also estimated by using Scherrer's equation with the reflection peak at 2θ of 27.36° . The average crystallite size increased slightly with time from 8.81 nm after 1.5 h and 9.55 nm after 6 h. The d -spacing of the reflection peak at 2θ of 27.36° was not changed throughout the polymerization. Aggregates of ribbon-like crystals with high crystallinity were formed in the early stage in the polymerization, and then they grew up to the fibers with maintaining the high crystallinity.

Oligomers left in LPF at 350°C were collected from the solution after 6 h, and analyzed by MALDI-TOF mass spectrometry. The spectrum and

the peak assignment are also shown in Figure 7(b) and Table II. The lower oligomers than those prepared in DBT were detected and this result indicates that the imidazole dimmers were phase-separated in LPF due to lower miscibility. The lower molecular

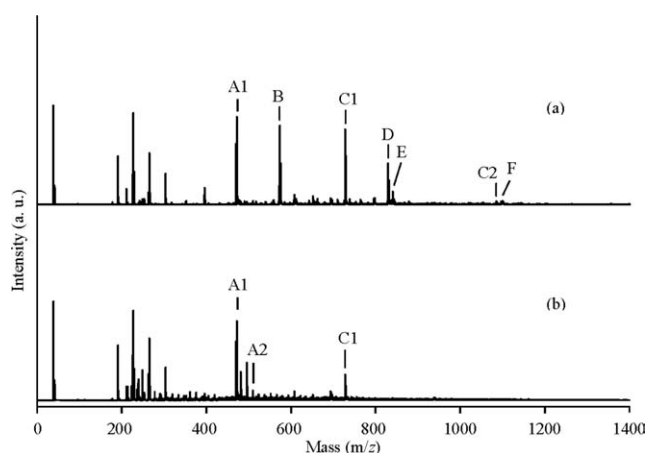
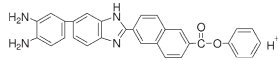
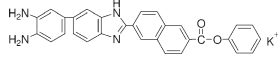
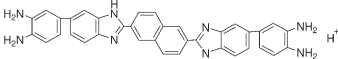
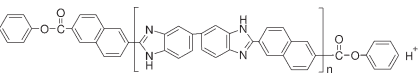
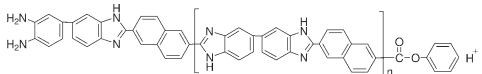
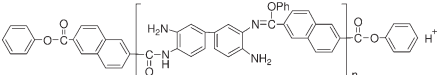
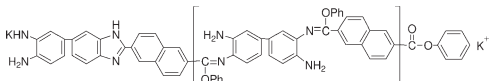
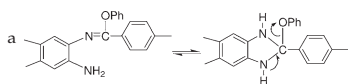


Figure 7 MALDI-TOF mass spectra of PNT-BBI oligomers collected from solution after 6 h polymerization in (a) DBT (run no. 8) and (b) LPF (run no. 4).

TABLE II
Assignments of Peaks in the MALDI-TOF Mass Spectra of Figure 7

Peak code	Mass (m/z)		Structure	n
	Measured	Calculated		
A1	470.92	471.55		-
A2	508.87	509.64		-
B	572.98	573.69		-
C1	727.01	727.81		1
C2	1085.50	1086.21		2
D	828.63	829.95		1
E ^a	838.68	839.94		1
F ^a	1094.50	1094.35		1



weight of the precipitated oligomers makes lower the freezing point of the oligomers leading to the induction of liquid-liquid phase separation rather than crystallization as previously reported.^{26,30} This might be a reason why the spherical aggregates were formed in LPF as above described.

CONCLUSIONS

As for PNT-BI, the aggregates of ribbon-like crystals were obtained in LPF. The size of ribbon-like crystals is 150 to 300 nm in thickness and 0.6 to 1.0 μm in width. The surface of ribbon-like crystals is rugged and covered with 100 to 250 nm of rice-like granules. As for PNT-BBI, although spherical aggregates of fine crystals were formed in LPF, the network structure of fibers having the diameter of 25 to 90 nm was mainly obtained in DBT with the yield of 52%. The fibers prepared in DBT had the highest molecular weight and they exhibited high crystallinity. The cyclized imidazole trimers were precipitated to form the crystal and then they were continuously supplied from solution to grow the crystals. The molecular weight increased by the polymerization on the surface of the crystals when they crystallized and in the crystals. This unique morphology resembled the nonwoven fabrics and it can be recognized as the nonwoven fab-

rics of the high-performance nanofibers. Only the plate-like crystals of PBP-BI were formed in all solvents, but PBP-BBI exhibited various morphologies depending on the solvent. Spheres were obtained in LPF, and both spheres and lath-like precipitates were obtained in DBT/LPF-50. The precipitates prepared in this study possessed very high crystallinity and the outstanding thermal stability.

References

- Cassidy, P. E. *Thermally Stable Polymers, Syntheses and Properties*; Marcel Dekker: New York, 1980.
- Korshak, V. V. *Heat-Resistant Polymers*; Israel Program for Scientific Translations: Jerusalem, 1971.
- Deimede, V.; Voyiatzis, G. A.; Kallitsis, J. K.; Qingfeng, L.; Bjerrum, N. J. *Macromolecules* 2000, 33, 7609.
- Li, Q.; He, R.; Jensen, J. O.; Bjerrum, N. *Fuel Cells* 2004, 4, 147.
- Hughes, C. E.; Haufe, S.; Angerstein, B.; Kalim, R.; Mahr, U.; Reiche, A.; Baldus, M. *J Phys Chem B* 2004, 108, 13626.
- Xiao, L.; Zhang, H.; Scanlon, E.; Ramanathan, L. S.; Choe, E. -W.; Rogers, D.; Apple, T.; Benicewicz, B. C. *Chem Mater* 2005, 17, 5328.
- Arunbabu, D.; Sannigrahi, A.; Jana, T. *J Phys Chem B* 2008, 112, 5305.
- Li, Q.; He, R.; Jensen, J. O.; Bjerrum, N. J. *Chem Mater* 2003, 15, 4896.
- Sumpter, B. G.; Noid, D. W.; Barnes, M. D.; Otaigbe, J. U. *Encyclopedia Nanosci Nanotechnol* 2004, 8, 873.
- Woodson, M.; Liu, J. *J Am Chem Soc* 2006, 128, 3760.

11. Zhong, W.; Wang, Y.; Yan, Y.; Sun, Y.; Deng, J.; Yang, W. *J Phys Chem B* 2007, 111, 3918.
12. Vogel, H.; Marvel, C. S. *J Polym Sci* 1961, 50, 511.
13. Iwakura, Y.; Uno, K.; Imai, Y. *J Polym Sci Part A: Gen Pap* 1964, 2, 2605.
14. Imai, Y.; Uno, K.; Iwakura, Y. *Makromol Chem* 1965, 83, 179.
15. Higgins, J.; Marvel, C. S. *J Polym Sci Part A: Polym Chem* 1970, 8, 171.
16. Gerber, A. H. *J Polym Sci Polym Chem Ed* 1973, 11, 1703.
17. Hedberg, F. L.; Marvel, C. S. *J Polym Sci Polym Chem Ed* 1974, 12, 1823.
18. Dudgeon, C. D.; Vogl, O. *J Polym Sci Polym Chem Ed* 1978, 16, 1831.
19. Neuse, E. W.; Loonat, M. S. *Macromolecules* 1983, 16, 128.
20. Ueda, M.; Sato, M.; Mochizuki, A. *Macromolecules* 1985, 18, 2723.
21. Neuse, E. W. *Adv Polym Sci* 1982, 47, 1.
22. Kanatzidis, M. G.; Wu, C. G.; Marcy, H. O.; Kannewurf, C. R. *J Am Chem Soc* 1989, 111, 4139.
23. Wu, C. G.; Kanatzidis, M. G.; Marcy, H. O.; DeGroot, D. C.; Kannewurf, C. R. *Polym Mater Sci Eng* 1989, 61, 969.
24. Kanatzidis, M. G.; Wu, C. G.; Marcy, H. O.; DeGroot, D. C.; Schindler, J. L.; Kannewurf, C. R.; Benz, M.; LeGoff, E. *ACS Symp Ser* 1992, 499, 194.
25. Husman, P.; Helminiak, T.; Adams, W. *ACS Symp Ser* 1980, 132, 203.
26. Nephew, J. B.; Nihei, T. C.; Carter, S. A. *Phys Rev Lett* 1998, 80, 3276.
27. Tran-Cong, Q.; Harada, A. *Phys Rev Lett* 1996, 76, 1162.
28. Kyu, T.; Lee, J. H. *Phys Rev Lett* 1996, 76, 3746.
29. Williams, R. J. J.; Rozenberg, B. A.; Pascault, J. P. *Adv Polym Sci* 1997, 128, 95.
30. Luo, K. *Eur Polym Mater* 2006, 42, 1499.
31. Wang, X.; Okada, M.; Matsushita, Y.; Furukawa, H.; Han, C. C. *Macromolecules* 2005, 38, 7127.
32. Yamashita, Y.; Kimura, K. In *Polymeric Materials Encyclopedia*; CRC Press: Boca Raton, 1996; p 8707.
33. Kimura, K.; Kohama, S.; Yamazaki, S. *Polym J* 2006, 38, 1005.
34. Kohama, S.; Gong, J.; Kimura, K.; Yamazaki, S.; Uchida, T.; Shimamura, K.; Kimura, K. *Polymer* 2008, 49, 1783.
35. Gong, J.; Kohama, S.; Kimura, K.; Yamazaki, S.; Kimura, K. *Polymer* 2008, 49, 3928.
36. Gong, J.; Uchida, T.; Yamazaki, S.; Kimura, K. *Macromol Chem Phys* 2010, 211, 2226.
37. Kimura, K.; Gong, J.; Kohama, S.; Yamazaki, S.; Uchida, T.; Kimura, K. *Polym J* 2010, 42, 375.
38. Gies, A. P.; Nonidez, W. K.; Anthamatten, M.; Cook, R. C.; Mays, J. W. *Rapid Commun Mass Spectrom* 19032002, 16.